Defence Technology 13 (2017) 188–199

Contents lists available at ScienceDirect

Defence Technology

journal homepage: www.elsevier.com/locate/dt

Validation of the NATO Armaments Ballistic Kernel for use in small-arms fire control systems

D. Corriveau*

Defence R&D Canada, 2459 De La Bravoure Rd., Quebec QC G3J 1X5, Canada

ARTICLE INFO

Article history:
Received 29 January 2017
Received in revised form
11 April 2017
Accepted 24 April 2017
Available online 27 April 2017

Keywords:
Aerodynamics
Ballistics
Trajectory
BALCO
NABK
Ballistic computer
Sniper system

ABSTRACT

In support for the development of a new small-arm ballistic computer based on the NATO Armaments Ballistic Kernel (NABK) for the Canadian snipers, DRDC Valcartier Research Centre was asked to carry out high-fidelity 6 degree-of-freedom (6-DOF) trajectory simulations for a set of relevant vignettes for the snipers, and to compare the direct fire 6-DOF simulation results with those obtained with the 4-DOF NATO Armaments Ballistic Kernel (NABK) adapted to simulate small-arm ammunition trajectories. To conduct this study, DRDC Valcartier Research Centre used BALCO v1.0b. This paper presents (1) the process and the methodology employed to carry out the sniper direct fire solution study, (2) the modeling and the simulation of the sniper projectile, the approach used in calculating the firing solutions, and the results of direct fire simulations for the sniper vignettes, and (3) an analysis of firing solutions obtained with the BALCO engine versus those of NABK. The work presented in this paper serves to validate the use of NABK for the new sniper ballistic computer.

1. Introduction

The development of the NABK started in the nineties in what is now called the NATO Land Capability Group 3 Sub-Group 2. Members of this group elected for a standard, generic, and layered set of software modules for ballistic processing [1]. The Ada computer language was selected given its wide acceptance and embedded application capability. The NABK was first released in 1995 for use in artillery and mortar technical fire control applications. It is currently used by more than ten NATO countries as the main ballistic engine for the artillery and mortar applications. The NABK is also planned for use by naval applications as well as in the next generation of fire support systems including guided artillery, mortars and direct fire applications such as fighting vehicles and tanks.

Although the NABK has been a very successful ballistic engine for various types of weapon systems and for the development of firing tables [2] [3], the small arms fire control for individual and crew served weapons ballistic solution is one area where the NABK is not well suited due to the unique requirements of the domain. Historically, fire control systems for small arms presented a unique environment and requirements to the developer of technical fire control systems. Small arms fire control systems are typically small in size which limited the available computer resources; CPUs are of lower power with correspondingly less processing capabilities; the amount of random access memory may also be limited. Operating systems used in small arms fire control systems are typically embedded real-time systems. This limits the choice of computer programming languages and compilers that support these systems and also places real-time requirements on the applications that run under the hardware and operating system. However, with the constant miniaturization of electronic components and the continually increasing computer power, the factors preventing the use of the NABK for small-arms fire control system have progressively been eliminated.

With today's smartphone platform, it was demonstrated by the Canadian snipers that the computer power of these devices was sufficient to run the NABK and instantly generate a ballistic solution for the snipers. Fig. 1 shows the Canadian snipers NABK ballistic computer kit with the various sensor connectors and power pack.

In this paper, the work performed to validate the use of NABK as a ballistic engine for the Canadian snipers ballistic computer is presented. Comparisons between the trajectory predicted by NABK and BALCO are presented for a typical 7.62 mm sniper projectile.

* Corresponding author.
E-mail address: daniel.corriveau@drdc-rddc.gc.ca.
Peer review under responsibility of China Ordnance Society

http://dx.doi.org/10.1016/j.dt.2017.04.006

Nomenclature

C_{D_0}	zero-yaw drag coefficient
C_{D_2}	quadratic-yaw drag coefficient
C_{D_4}	quartic-yaw drag coefficient
C_{L_α}	lift force coefficient
$C_{L_{\alpha_0}}$	linear lift force coefficient
$C_{L_{\alpha_3}}$	cubic lift force coefficient
C_{M_α}	pitching moment coefficient
C_{M_q}	pitch damping moment coefficient
C_{l_p}	spin damping moment coefficient
C_{N_q}	pitch damping force coefficient
$C_{Y_{p_\alpha}}$	Magnus force coefficient
C_{Mp_α}	Magnus moment coefficient
QE	quadrant elevation
SE	super elevation
$AzT - DA^T$	azimuth of fire (Coriolis on, wind on, bullet spin on)
DA^T	total drift angle (Coriolis on, wind on, bullet spin on)
$AzF^{\overline{C}}$	azimuth of fire (Coriolis off)
DA^C	drift angle due to Coriolis
$AzF^{\overline{CW}}$	azimuth of fire (Coriolis off, wind off)
DA^S	drift angle due to bullet spin
DA^W	drift due to wind
d	projectile reference diameter
p	projectile axial spin
q_t	total angular velocity
S	projectile reference area
V	projectile velocity
α_t	total angle of attack
ρ	air density
δ	$\sin\alpha_t$

Fig. 1. The Canadian snipers NABK ballistic computer kit with the various sensor connectors and power pack.

Various engagement scenarios are investigated to confirm that NABK performs well for different environmental conditions and firing directions. The comparison of the results obtained from the two ballistic engines are made and discussed.

2. NABK in brief

The NATO Armament Ballistic Kernel is a 4-DOF modified point mass model. This is a compromise between a simple point mass model and a computationally intensive 6-DOF model. NABK is based on the mathematical model defined by the NATO STANAG 4355 [4]: The Modified Point Mass and Point Mass Equations of Motion. In the modified point mass model, the effects due to the spin rate of a projectile are included contrary to a simple point mass model. Thus, the equilibrium yaw angle in both the lateral and trajectory plane is taken into account for calculation of the drift and drag. The 4-DOF modified point mass model is the algorithm implemented in trajectory simulation programs NABK. The trajectory integration is carried out using the Runge-Kutta-Fehlberg integration scheme. This is a fourth order numerical integration scheme. The projectile and the environment can be described with various levels of detail using the following models:

- Earth: flat (fixed gravity), spherical (STANAG 4355) or ellipsoidal (WGS84) Earth model;
- Atmosphere: standard atmosphere (ISO 2533-1975) or user-defined atmosphere, including a 1D or 3D wind field;
- Aerodynamics: axisymmetric projectiles, isolated control surfaces, aerodynamic coefficients described by polynomials;
- Inertia data: symmetric matrix of inertia;
- Base-burn and rocket assistance models (STANAG 4355);
- 5-DoF for fin stabilized rocket

3. BALCO in brief

BALCO is a 6/7-DoF trajectory simulation program based on the mathematical model defined by the NATO Standardization Recommendation 4618 [5] [6]. The primary goal of BALCO is to compute high-fidelity trajectories for both conventional and precision-guided projectiles. The 6-DoF model is used to describe the motion of single rigid bodies. The 7-DoF model allows the description of a projectile which consists of two coaxial rigid bodies that can spin independently. Actuators such as isolated control surfaces (e.g. fins or canards), thrusters or internal roll control devices can optionally be attached to the rigid body. Controlling the state of these actuators offers a control authority on the trajectory. The 6/7-DoF equations of motion can be expressed in three different frames, namely, body-fixed, zero roll and zero spin frames, depending on the context of the study. The trajectory integration is carried out using an accurate seventh-order Runge-Kutta scheme. The projectile, the environment and the optional guidance, navigation and control capabilities can be described with various levels of detail using the following models:

- Earth: flat (fixed gravity), spherical (STANAG 4355) or ellipsoidal (WGS84) Earth model;
- Atmosphere: standard atmosphere (ISO 2533-1975) or user-defined atmosphere, including a 1D or 3D wind field;
- Aerodynamics: axisymmetric or non-axisymmetric projectiles, isolated control surfaces, aerodynamic coefficients described by multidimensional look-up tables or polynomials;
- Inertia data: symmetric or asymmetric matrix of inertia, user-defined timedependent inertia;
- Thrusters: user-defined time-dependent 3D vector thrusts;
- Base-burn and rocket assistance models (STANAG 4355);
- Embedded actuators (open- or closed-loop flight control): isolated control surfaces, thrusters and internal rolling moment for dual-spin bodies;

- Guidance, navigation and control models implemented as external functions using a common communication interface (closed-loop flight control).

4. Sniper ammunition model

The sniper ammunition of used for this project is the NATO 7.62 × 51 mm, OTBT (Open Tip Boat Tail), 168 gr, Match, which is simply referred to in this paper as the C175. The aerodynamic model for this round was developed using PRODAS (Fig. 2) combined with some experimental firing radar traces.

The aerodynamic coefficients generated in PRODAS that are actual inputs to the BALCO model and NABK model are as follows: C_{D_0}, C_{D_2}, C_{D_4}, $C_{L_{\alpha_0}}$, $C_{L_{\alpha_3}}$, C_{M_α}, C_{M_q}, C_{l_p}, C_{N_q}, $C_{Y_{p\alpha}}$ and C_{Mp_α}.

The coefficients C_{D_0}, C_{D_2} and C_{D_4} are used to calculate to total drag coefficient taking into account the projectile's yaw as follows

$$C_D = C_{D_0} + C_{D_2}\delta^2 + C_{D_4}\delta^4 \tag{1}$$

where $\delta = \sin \alpha_t$. α_t is the total angle of attack.

The lift force coefficient C_{L_α} is often nonlinear as the yaw level varies. This behaviour is captured using the following relationship

$$C_{L_\alpha} = C_{L_0} + C_{L_3}\delta^2. \tag{2}$$

The pitching moment is directly related to the lift force. For small caliber projectiles, the pitching moment is usually positive. Therefore, if the nose of the projectile rises above the trajectory, the pitching moment will act as to increase the yaw angle. The pitching moment relates to the pitching moment coefficient as follows

$$Pitching\ \ Moment = \frac{1}{2}\rho V^2 S d C_{M_\alpha} \sin \alpha_t. \tag{3}$$

The pitch damping moment arises from the attenuation of pitching motion of a projectile due to the air resistance. The pitch damping moment relates to the pitch damping moment coefficient as follows:

$$Pitch\ Damping\ Moment = \frac{1}{2}\rho V^2 S d\left(\frac{q_t d}{V}\right) C_{M_q} \tag{4}$$

where q_t is the total angular velocity.

Similarly, the pitch damping force relates to the pitch damping force coefficient as follows

$$Pitch\ Damping\ Force = \frac{1}{2}\rho V^2 S d\left(\frac{q_t d}{V}\right) C_{N_q}. \tag{5}$$

The spin damping moment opposes the spin of the projectile. It relates to the spin damping coefficient as follows

$$Spin\ Damping\ Moment = \frac{1}{2}\rho V^2 S d\left(\frac{pd}{V}\right) C_{lp}. \tag{6}$$

The Magnus force arises from the unequal pressures distribution on either side of a spinning body. This is the result of the viscous interaction between the spinning projectile body and the fluid. The Magnus force relates to the Magnus force coefficient as follows

$$Magnus\ Force = \frac{1}{2}\rho V^2 S\left(\frac{pd}{V}\right) C_{Yp\alpha} \sin \alpha_t. \tag{7}$$

Similarly, the Magnus moment is a function of the Magnus moment coefficient given as

$$Magnus\ Moment = \frac{1}{2}\rho V^2 S d\left(\frac{pd}{V}\right) C_{Mp\alpha} \sin \alpha_t. \tag{8}$$

5. Direct fire simulation comparison study

In order to compare the direct fire solution of NABK with that obtained from the 6-DOF trajectory simulation code BALCO a set of 20 vignettes was developed. These vignettes represent typical firing conditions that could be encountered around the world by the snipers. The vignette locations are shown in the map presented in Fig. 3.

The vignettes spread locations all over the world, as shown as squares on the simple map of Fig. 3. The vignettes also cover a relatively large range of air temperatures (from −40° C to 49° C), air pressure (from 98.1 kPa to 103.6 kPa), relative humidity (from 0 to 100%), wind speed (from 0 to 30 km/h), gun altitude (from 0 to 3600 m), gun range (from 300 to 1200 m), angles of sight (from −533 to 355 mils), and propellant temperature (from −20° C to 70° C). The vignettes data are presented in Table 1 to Table 3.

A vignette is a simulation scenario composed of defining elements. Typically, one finds the following parameters in a vignette: geo-location and altitude of the shooter, shooter-target range, altitude of target, temperature and barometric pressure at the shooter location, relative humidity at the shooter position, wind speed and direction, rifle azimuth from the North, and shooter-target slant angle.

Simulation involves numerically running a model of the projectile, namely solving the equations of motion over time, preferably in the BALCO environment, under the conditions of interest, and then collecting the results, such as projectile position and velocity versus time, to cite a few.

Briefly, the projectile model is characterized by the usual aerodynamic parameters [7]. The parameters are obtained with PRODAS, leveraging the knowledge of the geometry of the projectile. Furthermore, some radar traces were used to refine the aerodynamic model. The PRODAS aerodynamic model is implemented in BALCO. The 6-DOF numerical simulations are run in BALCO. The trajectory of the projectile is obtained through the solution of the equations of motion; namely, a solution to a number of differential equations calculated with classical Runge-Kutta methods.

As a minimum the following results were collected on the rifle and projectile: quadrant elevation (QE), super elevation (SE), time

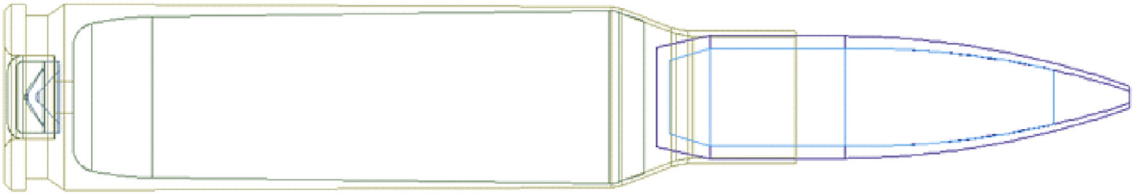

Fig. 2. C175 representation (cartridge and projectile) in PRODAS.

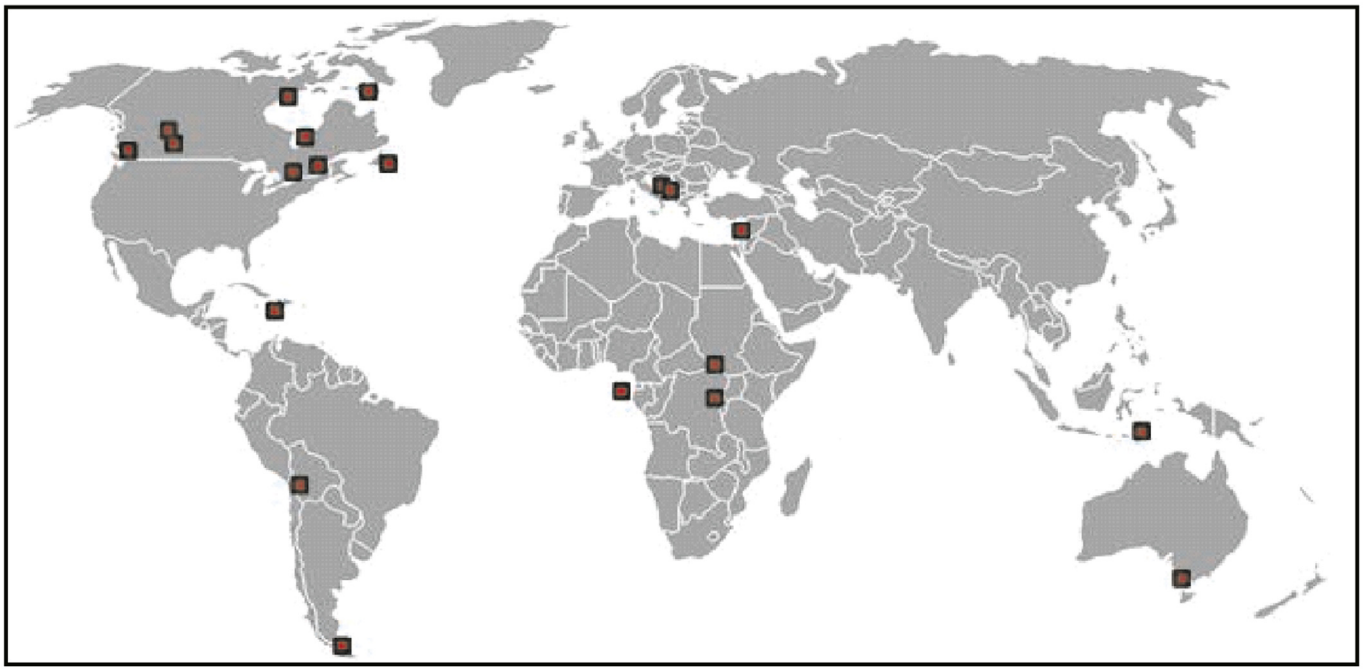

Fig. 3. Locations of the vignettes.

Table 1
Original vignettes 1 to 7.

Variables		Unit	SET#1	SET#2	SET#3	SET#4	SET#5	SET#6	SET#7
Temperature	Outside	°C	−40	−37	−32	−27	−22	−18	−13
	Ammunition	°C	−20	−16	−11	−6	−1	4	8
Barometric pressure		kPa	103.658	98.146	98.874	100.135	103.692	102.743	99.176
Altitude above sea lever (Information only)		m	50	300	2000	380	215	100	693
Relative humidity		%RH	36	50	88	65	30	43	81
Wind direction		(°)	320	45	76	285	230	205	0
		Mil	5689	800	1351	5067	4089	3644	0
		($km \cdot h^{-1}$)	30.0	15.0	28.0	29.0	18.0	25.0	7.0
Wind speed		($m \cdot s^{-1}$)	8.33	4.17	7.78	8.06	5.0	6.94	1.94
Azimuth from north		(°)	180	320	45	70	340	250	90
		Mil	3200	5689	800	1244	6044	4444	1600
Slant angle		(°)	−0.5	−2.0	20.0	−3.0	−12.0	−6.0	−3.0
Geo-location	Latitude	(°)Decimal	N63.720982	N62.811666	N50.097100	N56.737700	N53.785010	N45.448112	N53.522783
	Longitude	(°)Decimal	W68.526707	W92.109439	W122.893281	W111.382230	W77.454858	W75.693011	W113.623052
Range to target		m	600	1200	920	825	780	400	450

Table 2
Original vignettes 8 to 15.

Variables		Unit	SET#8	SET#9	SET#10	SET#11	SET#12	SET#13	SET#14	SET#15
Temperature	Outside	°C	−8	−3	2	6	11	15	21	25
	Ammunition	°C	13	18	23	27	32	15	42	46
Barometric pressure		kPa	101.125	99.526	101.870	100.745	102.437	101.325	101.860	98.525
Altitude above sea lever (Information only)		m	300	180	855	3656	600	0	20	150
Relative humidity		%RH	60	97	100	30	45	0	100	73
Wind direction		(°)	320	180	165	270	325	0	195	90
		Mil	5689	3200	2933	4800	5778	0	3467	1600
		($km \cdot h^{-1}$)	10.00	13.00	30.24	8.00	17.00	0.00	26.00	22.00
Wind speed		($m \cdot s^{-1}$)	2.78	3.61	8.40	2.22	4.72	0.00	7.22	6.11
Azimuth from north		(°)	280	210	80	200	180	90	160	165
		Mil	4978	3733	1422	3556	3200	1600	2844	2933
Slant angle		(°)	−10.0	−30.0	1.0	0.0	15.0	10.0	−1.0	−5.0
Geo-location	Latitude	(°)Decimal	N44.039417	S52.875813	N33.235242	S20.317544	N43.834465	N0.359936	S38.290897	N47.539281
	Longitude	(°)Decimal	E16.190329	W69.344587	E35.927653	W66.962786	E18.352919	E6.552225	E144.610795	W52.690256
Range to target		m	375	300	540	1000	650	1100	500	580

Table 3
Original vignettes 16 to 20.

Variables		Unit	SET#16	SET#17	SET#18	SET#19	SET#20
Temperature	Outside	°C	30	35	40	44	49
	Ammunition	°C	51	56	61	65	70
Barometric pressure		kPa	102.600	100.400	103.237	101.715	99.934
Altitude above sea lever (Information only)		m	120	105	603	1640	110
Relative humidity		%RH	80	98	30	87	93
Wind direction		(°)	223	58	94	317	138
		Mil	3964	1031	1671	5636	2453
		($km \cdot h^{-1}$)	5.0	9.0	4.0	3.0	27.0
Wind speed		($m \cdot s^{-1}$)	1.39	2.50	1.11	83.00	7.50
Azimuth from north		(°)	170	120	70	110	325
		Mil	3022	2133	1244	1956	5778
Slant angle		(°)	−1.0	−7.0	−1.0	−6.0	−4,0
Geo-location	Latitude	(°)Decimal	N46.749847	N18.234800	N7.729556	S1.619056	S9.209517
	Longitude	(°)Decimal	W71.292136	W72.478836	E27.995508	E29.242086	E124.321358
Range to target		m	435	670	700	800	425

of flight, velocity at impact, transonic entry distance, maximum ordinate, azimuth of fire (with and without Coriolis effect, and with and without wind), and drift angle (due to projectile spin, Coriolis effect, and wind, and due to a combination of those factors). These parameters are defined in the report and their values obtained for the various vignettes are presented.

The following elements are of particular importance for the sniper: super elevation, drift angle, and range to transonic entry. And as such, these variables are collected during the simulations.

6. Approach

The steps in the DRDC simulation study are shown in Fig. 5. The six steps are carried out for each vignette. Then, results of the simulations are collected, metrics are calculated, and differences between NABK and BALCO are quantified and analysed.

Once the projectile data is entered for a vignette, the information is valid and fixed for all vignettes. The vignette specific information on geometry, meteorological conditions, wind parameters, and geo location are extracted from the Excel table, and entered into the BALCO input script file. Using the tabular data associated with a vignette, one fills out the BALCO input file as follows:

- $ISO_Atmosphere_Correction_Data is entered as the triplet altitude [m], temperature [K], and pressure [Pa],
- $Wind_Data is entered as components in a Cartesian frame, with one component along $x1$ (down-range), followed by a component along $x2$ (vertical, always zero here), and finally a component along $x3$ (cross-range),
- $Longitude_Latitude_Azimuth is entered as longitude (deg) and latitude (deg), complying with the sign convention used in this study, and as azimuth (deg) of fire (specifically, the azimuth from the North entry of the vignette table data), in this order,
- $Initial_Position is entered as down range (m) of zero, height (m) above sea level as given in the vignette table, and cross range (m) of zero, in this order, as the position of the shooter (gun).

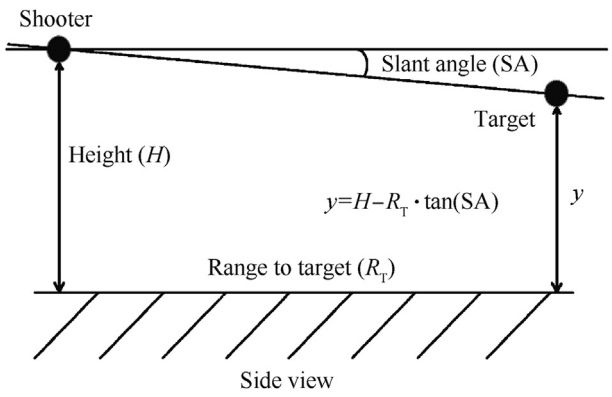

Fig. 4. Example of target height calculation.

Target location is determined from the geometry of the vignette, using the vignette information on the slant angle, the height of the shooter, and the range to target. Actually, target height from sea level is critical, as it serves in the evaluation of the drift angle. Fig. 4 presents a generic geometry and basic calculations to obtain target height (y) from vignette parameters.

The next step pertains to setting the QE, the initial conditions, the stopping conditions, and the format of the simulation output. Obtaining the QE value, by trial and error, that results in the projectile hitting the target is the iterative part of the approach. Using the tabular data associated with a vignette:

- $Initial_Time is set to zero,
- $Initial_Velocity is entered as the triplet of magnitude (m/s) of the projectile at firing obtained from the NABK data, followed by the deflection angle set to zero, and the elevation angle (QE) as the estimated value to reach the target,
- $Initial_Angular_Position is entered as 0, 0, and 0 (for aerodynamic roll angle, total angle of attack, and roll angle),
- $Initial_Angular_Velocity is entered as the spin rate (rad/s) of the projectile obtained with PRODAS (with NABK supplied projectile velocity magnitude at firing), and followed by zero pitch rate, and zero yaw rate,
- Stopping condition is $Trajectory_Limit entered as the range to target value for the vignette,
- $Print_Time_Step is entered as the appropriate value that gives enough increment in the output, and may vary from 0.0005 s to 0.01 s depending on the vignette and output results.

With the aforementioned key parameter values identified and set, the simulations of a vignette may be run, as shown in Fig. 5.

As for the trial and error process associated with the QE value, a simulation is first run with the originally guessed QE value. One obvious choice for the first guess on QE is the NABK QE value, which is available. The projectile location obtained at the downrange

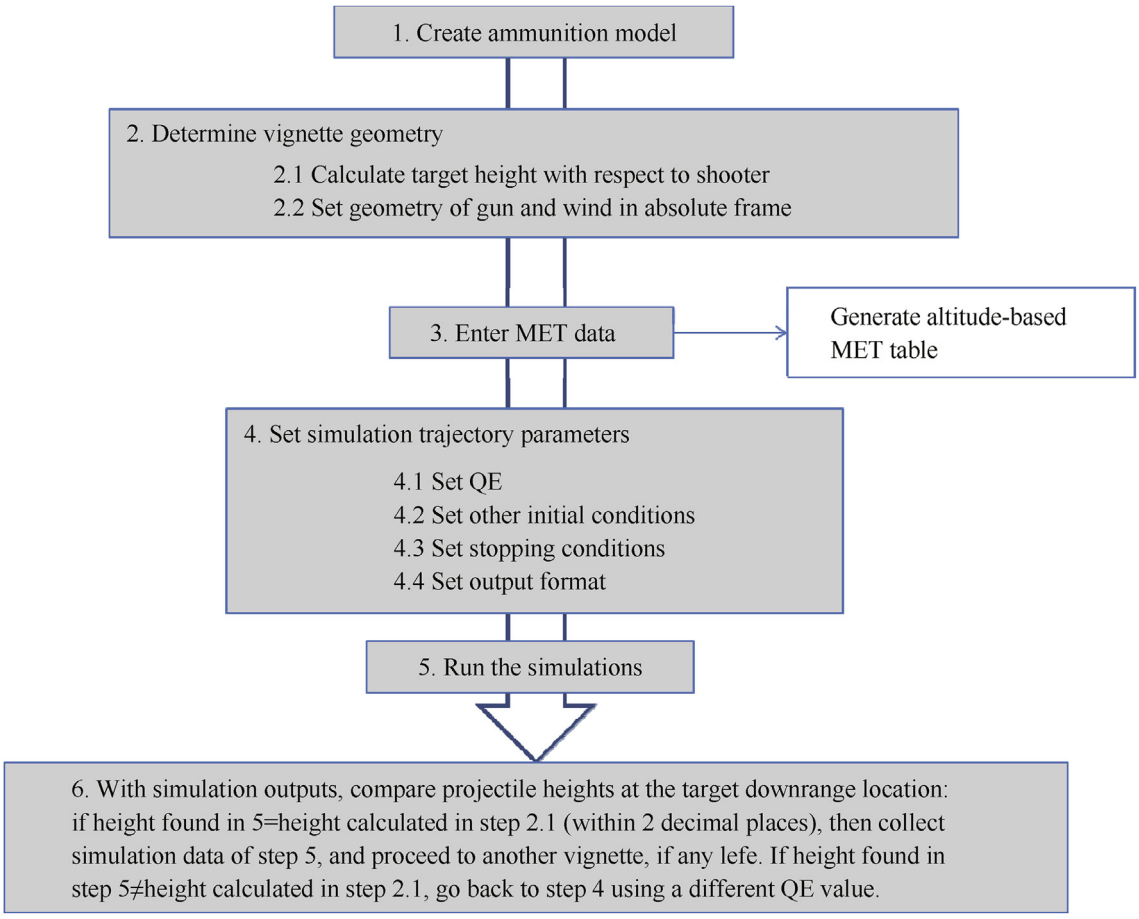

Fig. 5. Main steps in direct fire simulation study.

target position is then compared with that expected from the geometry of the shooter-target, with a computation as shown in Fig. 4. If the projectile does not end up at the correct target altitude within 2 decimal places in units of meters, at the target downrange value location, the QE is set to another value, and the simulation is run again. The process is repeated until a satisfactory projectile altitude at target is obtained.

Note that several simulations are run for a given vignette and fixed (final) QE value to allow for post-processing calculations that isolate the effects of three variables on the drift angle: Coriolis effect, wind, and bullet spin.

7. Results

The results obtained with BALCO and NABK for the sniper vignettes are presented in Table 4 to Table 10. The variables used for performance evaluation and other variables, as required by the snipers, are shown in the tables. The columns are arranged such that the NABK and BALCO results are presented side by side for each vignette.

Other variables of interest found in the results tables are as follows: projectile's time of flight, muzzle velocity (MV), velocity at impact (actually, when projectile is closest to target), transonic entry distance, maximum ordinate, and range to maximum ordinate. Range to maximum ordinate is the distance from the gun position to the horizontal coordinate of the location of the projectile when it reaches its highest altitude.

8. NABK versus BALCO trajectory comparisons

The objective of the verification and validation process is to demonstrate the accuracy of NABK solution so that it may be used with confidence in a ballistic computer for the snipers. According to AIAA guidelines [8], the verification process determines if the programming and computational implementation of the conceptual model is correct. It examines the mathematics in the model through comparison with exact analytical results and checks for computer programming errors. As for the validation process, it determines if the computational simulation agrees with physical reality through comparison with experimental results.

To compare the trajectory algorithms of NABK with that of BALCO, one may state a number of observations on the results using Table 11 to Table 14, in particular those tables featuring the differences in key variables. A detailed explanation of the results obtained with NABK is outside the scope of the analysis.

For each vignette, the difference in NABK and BALCO QE inputs is smaller than or equal to 0.012°. The maximum value of 0.012° is obtained with vignette 19. If one omits vignette 19, the largest difference in QE is smaller than or equal to 0.0098°. The same observations can be made for SE.

The maximum difference in magnitude of velocity at impact between NABK and BALCO for all vignettes is 2%. The maximum is obtained with vignette 19. If one discards this vignette, the maximum difference falls to 0.6%.

The relatively large difference in NABK and BALCO QE inputs observed for vignette 19 can be explained in terms of the virtual

Table 4
Results for vignettes 1 and 2.

Variables	Unite	V1 NABK	V1 BALCO	V2 NABK	V2 BALCO
Wind speed	knots	16	16	8	8
Height of *T*gt (rel. gun)	m	−5.236120674	−5.236120674	−41.90492339	−41.90492339
Slant angle	gun mils	−8.888888889	−8.888888889	−35.55555556	−35.55555556
Azimuth to target	gun mils	3200	3200	5689	5689
Target altitude	m	45	45	258	258
Quadrant elevation	gun mils	−1.34	−1.3138	−7.71	−7.7867
Quadrant elevation	mrads	−1.31	−1.2898	−7.57	−7.6445
Quadrant elevation	(°)	−0.08	−0.0739	−0.43	−0.4380
Super elevation	(°)	0.42	0.4261	1.57	1.5620
Super elevation	**mrads**	**7.41**	**7.4368**	**27.34**	**27.2620**
Azimuth of fire	gun mils	3202.66	3202.6893	5693.45	5693.5925
Azimuth of fire	mrads	3144.20	3144.2329	5589.53	5589.6714
Total drift angle	gun mils	−2.66	−2.6893	−4.56	−4.5925
Total drift angle (Coriolis on, wind on, spin on)	**mrads**	**−2.61**	**−2.6402**	**−4.48**	**−4.51**
Time of flight	s	1.08	1.0777	3.07	3.05
MV corrected for PT	($m \cdot s^{-1}$)	790.70	790.7040	792.20	792.20
Velocity at Impact	($m \cdot s^{-1}$)	391.77	392.0360	253.33	254.37
Transonic entry distance	m	None	None	685.12	603 DR($v = 408$ m/s)
Transonic exit distance	m	None	None	None	
Maximum ordinate	m	0.00	0.0000	0.00	0.0000
Range to max ordinate	m	0.00	0.0000	0.00	0.0000
Azimuth of fire (Coriolis off)	gun mils	3202.722	3202.75	5693.61	5693.76
Azimuth of fire (Coriolis off)	mrads	3144.264971	3144.294718	5589.69051	5589.832274
Drift angle due to coriolis	gun mils	−0.06	−0.0630	−0.16	−0.1639
Drift angle due to coriolis	mrads	−0.06	−0.0618	−0.16	−0.1609
Azimuth of fire (Coriolis off, wind off)	gun mils	3199.83	3199.8315	5688.24	5688.33
Azimuth of fire (Coriolis off, wind off)	mrads	3141.42	3141.43	5584.42	5584.50
Drift angle due to bullet spin	gun mils	0.17	0.1685	0.65	0.67
Drift angle due to bullet spin	mrads	0.17	0.1654	0.63	0.66
Drift due to wind	gun mils	−2.77	−2.7948	−5.04	−5.10
Drift due to wind	mrads	−2.72	−2.7438	−4.95	−5.01

Table 5
Results for vignettes 3, 4 and 5.

Variables	Unite	V3 NABK	V3 BALCO	V4 NABK	V4 BALCO	V5 NABK	V5 BALCO
Wind speed	knots	15	15	16	16	10	10
Height of *T*gt (rel. gun)	m	334.852616	334.8526155	−43.236418	−43.23641791	−165.79412	−165.7941181
Slant angle	gun mils	355.555556	355.5555556	−53.333333	−53.33333333	−213.33333	−213.3333333
Azimuth to target	gun mils	800	800	1244	1244	6044	6044
Target altitude	m	2335	2335	337	337	49	49
Quadrant elevation	gun mils	370.136	370.3108	−41.07	−41.0133	−201.79	−201.6887
Quadrant elevation	mrads	363.38	363.5518	−40.32	−40.2647	−198.11	−198.0074
Quadrant elevation	(°)	20.82	20.83	−2.31	−2.31	−11.35	−11.345
Super elevation	(°)	0.82	0.8300	0.69	0.6930	0.65	0.65
Super elevation	**mrads**	**14.31**	**14.4862**	**12.04**	**12.0951**	**11.33**	**11.43**
Azimuth of fire	gun mils	803.745	803.7984	1240.38	1240.03440000000	6040.29	6039.94370000000
Azimuth of fire	mrads	789.07	789.13	1217.74	1217.40	5930.04	5929.70
Total drift angle	gun mils	−3.75	−3.7984	4.06	3.9656	4.15	4.0563
Total drift angle (Coriolis on, wind on, spin on)	**mrads**	**−3.68**	**−3.60**	**3.99**	**3.89**	**4.07**	**3.98**
Time of flight	s	2.235	2.234	1.66	1.66	1.59	1.60
MV corrected for PT	($m \cdot s^{-1}$)	794.135	794.135	796.14	796.14	798.21	798.21
Velocity at impact	($m \cdot s^{-1}$)	272.966	273.25	320.14	319.45	320.66	319.94
Transonic entry distance	m	642.06	561 DR($v = 408$ m/s)	674.11	622 DR($v = 408$ m/s)	636.90	592 DR($v = 408$ m/s)
Transonic exit distance	m	None		None		None	
Maximum ordinate	m	334.853	335	0.00	0.0000	0.00	0.0000
Range to max ordinate	m	920	920	0.00	0.0000	0.00	0.0000
Azimuth of fire (Coriolis off)	gun mils	803.83	803.8789	1240.47	1240.12	6040.38	6040.04
Azimuth of fire (Coriolis off)	mrads	789.153348	789.2062646	1217.82759	1217.486534	5930.13312	5929.791673
Drift angle due to coriolis	gun mils	−0.08	−0.08	−0.09	−0.09	−0.09	−0.09
Drift angle due to coriolis	mrads	−0.08	−0.08	−0.09	−0.09	−0.09	−0.09
Azimuth of fire (Coriolis off, wind off)	gun mils	799.59	799.59	1244.16	1243.72	6044.18	6043.73
Azimuth of fire (Coriolis off, wind off)	mrads	785.00	784.99	1221.45	1221.02	5933.86	5933.42
Drift angle due to bullet spin	gun mils	0.41	0.41	0.28	0.28	0.27	0.27
Drift angle due to bullet spin	mrads	0.40	0.40	0.28	0.28	0.26	0.26
Drift due to wind	gun mils	−4.08	−4.13	3.86	3.77	3.98	3.88
Drift due to wind	mrads	−4.00	−4.05	3.79	3.70	3.90	3.81

temperature. NABK simulations rely on the virtual temperature, which takes into account the relative humidity in the air. For most vignettes, the difference between the air temperature and the virtual temperature was relatively small or non-existent, therefore

Table 6
Results for vignettes 6, 7 and 8.

Variables	Unite	V6 NABK	V6 BALCO	V7 NABK	V7 BALCO	V8 NABK	V8 BALCO
Wind speed	knots	13	13	4	4	5	5
Height of *T*gt (rel. gun)	m	−42.041694	−42.04169411	−23.583501	−23.58350068	−66.122618	−66.12261777
Slant angle	gun mils	−106.66667	−106.6666667	−53.333333	−53.33333333	−177.77778	−177.7777778
Azimuth to target	gun mils	4444	4444	1600	1600	4978	4978
Target altitude	m	58	58	669	669	234	234
Quadrant elevation	gun mils	−102.30	−102.2612	−48.64	−48.6222	−174.02	−173.9910
Quadrant elevation	mrads	−100.44	−100.3947	−47.75	−47.7347	−170.84	−170.8152
Quadrant elevation	(°)	−5.75	−5.75	−2.74	−2.74	−9.79	−9.79
Super elevation	(°)	0.25	0.25	0.26	0.27	0.21	0.21
Super elevation	**mrads**	**4.28**	**4.32**	**4.61**	**4.63**	**3.69**	**3.72**
Azimuth of fire	gun mils	4442.95	4442.45380000000	1599.22	1599.25590000000	4978.11	4978.37020000000
Azimuth of fire	mrads	4361.86	4361.37	1570.03	1570.07	4887.25	4887.50
Total drift angle	gun mils	1.49	1.5462	0.78	0.7441	−0.33	−0.37
Total drift angle (Coriolis on, wind on, spin on)	**mrads**	**1.46**	**1.52**	**0.77**	**0.73**	**−0.32**	**−0.36**
Time of flight	s	0.62		0.70	0.70	0.57	0.57
MV corrected for PT	($m \cdot s^{-1}$)	800.36	800.36	802.12	802.12	804.39	804.39
Velocity at impact	($m \cdot s^{-1}$)	527.84	527.28	515.20	516.62	553.62	553.49
Transonic entry distance	m	None	None	None	None	None	None
Transonic exit distance	m	None		None		None	
Maximum ordinate	m	0.00	0.0000	0.00	0.0000	0.00	0.0000
Range to max ordinate	m	0.00	0.0000	0.00	0.0000	0.00	0.0000
Azimuth of fire (Coriolis off)	gun mils	4442.98	4442.48	1599.26	1599.29	4978.14	4978.40
Azimuth of fire (Coriolis off)	mrads	4361.88542	4361.397977	1570.06689	1570.103507	4887.27752	4887.531691
Drift angle due to coriolis	gun mils	−0.03	−0.03	−0.04	−0.04	−0.03	−0.03
Drift angle due to coriolis	mrads	−0.03	−0.03	−0.04	−0.04	−0.03	−0.03
Azimuth of fire (Coriolis off, wind off)	gun mils	4444.35	4443.91	1599.90	1599.90	4977.70	4977.92
Azimuth of fire (Coriolis off, wind off)	mrads	4363.23	4362.80	1570.70	1570.70	4886.85	4887.06
Drift angle due to bullet spin	gun mils	0.09	0.09	0.10	0.10	0.08	0.08
Drift angle due to bullet spin	mrads	0.09	0.09	0.10	0.10	0.08	0.08
Drift due to wind	gun mils	1.43	1.49	0.72	0.68	−0.38	−0.42
Drift due to wind	mrads	1.40	1.46	0.70	0.67	−0.37	−0.41

Table 7
Results for vignettes 9, 10 and 11.

Variables	Unite	V9 NABK	V9 BALCO	V10 NABK	V10 BALCO	V11 NABK	V11 BALCO
Wind speed	knots	7	7	16	16	4	4
Height of *T*gt (rel. gun)	m	−173.20508	−173.2050808	9.42573506	9.425735061	0	0
Slant angle	gun mils	−533.33333	−533.3333333	17.7777778	17.77777778	0	0
Azimuth to target	gun mils	3733	3733	1422	1422	3556	3556
Target altitude	m	7	7	864	864	3656	3656
Quadrant elevation	gun mils	−530.10	−530.0778	23.38	23.4311	16.05	16.1778
Quadrant elevation	mrads	−520.43	−520.4026	22.96	23.0034	15.76	15.8825
Quadrant elevation	(°)	−29.82	−29.82	1.32	1.32	0.90	0.91
Super elevation	(°)	0.18	0.18	0.32	0.32	0.90	0.91
Super elevation	**mrads**	**3.17**	**3.20**	**5.50**	**5.55**	**15.76**	**15.88**
Azimuth of fire	gun mils	3732.89	3732.55	1425.20	1425.05	3556.951	3557.53
Azimuth of fire	mrads	3664.76	3664.42	1399.19	1399.04	3492.03	3492.60
Total drift angle	gun mils	0.44	0.45	−2.98	−3.05	−1.40	−1.53
Total drift angle (Coriolis on, wind on, spin on)	**mrads**	**0.43**	**0.44**	**−2.93**	**−3.00**	**−1.37**	**−1.50**
Time of flight	s	0.50	0.50	0.87	0.87	2.10	2.10
MV corrected for PT	($m \cdot s^{-1}$)	806.73	806.73	809.14	809.14	811.12	811.12
Velocity at impact	($m \cdot s^{-1}$)	584.98	584.43	474.20	474.64	308.12	307.99
Transonic entry distance	m	None	None	None	None	699.54	685 DR($v = 408$ m/s)
Transonic exit distance	m	None		None		None	
Maximum ordinate	m	0.00	0.0000	9.43	9.40	5.52	5.70
Range to max ordinate	m	0.00	0.0000	540.00	540.00	581.22	590.00
Azimuth of fire (Coriolis off)	gun mils	3732.85	3732.52	1425.23	1425.08	3556.91	3557.49
Azimuth of fire (Coriolis off)	mrads	3664.71692	3664.389407	1399.21824	1399.072847	3491.98626	3492.554695
Drift angle due to Coriolis	gun mils	0.04	0.04	−0.03	−0.03	0.04	0.04
Drift angle due to Coriolis	mrads	0.04	0.03	−0.03	−0.03	0.04	0.04
Azimuth of fire (Coriolis off, wind off)	gun mils	3733.26	3732.9304	1422.10	1421.87	3555.21	3555.65
Azimuth of fire (Coriolis off, wind off)	mrads	3665.12	3664.80	1396.14	1395.92	3490.32	3490.75
Drift angle due to bullet spin	gun mils	0.07	0.07	0.13	0.13	0.35	0.35
Drift angle due to bullet spin	mrads	0.07	0.07	0.12	0.12	0.34	0.35
Drift due to wind	gun mils	0.33	0.34	−3.08	−3.15	−1.79	−1.93
Drift due to wind	mrads	0.33	0.34	−3.02	−3.09	−1.76	−1.89

had a minor impact on performance of the projectile. However, with vignette 19, one has a scenario with a very high temperature and high level of humidity. For vignette 19, the virtual temperature was 53.6 deg C as compared with 44 deg C for the air temperature.

Table 8
Results for vignettes 12, 13 and 14.

Variables	Unite	V12 NABK	V12 BALCO	V13 NABK	V13 BALCO	V14 NABK	V14 BALCO
Wind speed	knots	9	9	0	0	14	14
Height of *T*gt (rel. gun)	m	174.1669751	174.1669751	193.959679	193.9596788	−8.7275325	−8.727532464
Slant angle	gun mils	266.6666667	266.6666667	177.777778	177.7777778	−17.777778	−17.77777778
Azimuth to target	gun mils	3200	3200	1600	1600	2844	2844
Target altitude	m	774	774	194	194	11	11
Quadrant elevation	gun mils	274.76	274.8087	197.23	197.2976	−12.81	−12.8000
Quadrant elevation	mrads	269.74	269.7928	193.63	193.6965	−12.57	−12.5664
Quadrant elevation	(°)	15.46	15.46	11.09	11.10	−0.72	−0.72
Super elevation	(°)	0.46	0.46	1.09	1.10	0.28	0.28
Super elevation	**mrads**	**7.94**	**7.99**	**19.09**	**19.16**	**4.88**	**4.89**
Azimuth of fire	gun mils	3201.14	3201.18	1599.57	1599.56	2845.71	2845.27
Azimuth of fire	mrads	3142.71	3142.75	1570.37	1570.36	2793.77	2793.34
Total drift angle	gun mils	−1.14	−1.18	0.43	0.44	−1.26	−1.27
Total drift Angle (Coriolis on, wind on, spin on)	**mrads**	**−1.12**	**−1.15**	**0.42**	**0.43**	**−1.24**	**−1.25**
Time of flight	s	1.15	1.15	2.47	2.47	0.77	0.77
MV corrected for PT	$(m\cdot s^{-1})$	813.66	813.66	805.32	805.32	818.94	818.94
Velocity at impact	$(m\cdot s^{-1})$	420.22	420.00	298.25	298.32	513.72	513.48
Transonic entry distance	m	None	None	686.97	681 DR($v = 408$ m/s)	None	None
Transonic exit distance	m	None		None		None	
Maximum Ordinate	m	174.17	174.16	193.96	193.94	0.00	0.0000
Range to max ordinate	m	650.00	650.00	1100.00	1100.00	0.00	0.0000
Azimuth of fire (Coriolis off)	gun mils	3201.21	3201.24	1599.57	1599.56	2845.67	2845.24
Azimuth of fire (Coriolis off)	mrads	3142.779587	3142.81277	1570.36927	1570.362885	2793.73293	2793.303322
Drift angle due to coriolis	gun mils	−0.07	−0.07	0.00	0.00	0.03	0.03
Drift angle due to coriolis	mrads	−0.07	−0.07	0.00	0.00	0.03	0.03
Azimuth of Fire (Coriolis off, wind off)	gun mils	3199.83	3199.83	1599.57	1599.56	2844.34	2843.89
Azimuth of Fire (Coriolis off, wind off)	mrads	3141.43	3141.42	1570.37	1570.36	2792.42	2791.99
Drift Angle due to bullet spin	gun mils	0.17	0.17	0.43	0.44	0.11	0.11
Drift Angle due to bullet spin	mrads	0.17	0.17	0.43	0.43	0.10	0.10
Drift due to wind	gun mils	−1.24	−1.28	−0.01	0.00	−1.40	−1.41
Drift due to wind	mrads	−1.22	−1.26	−0.01	0.00	−1.37	−1.38

Table 9
Results for vignettes 15, 16 and 17.

Variables	Unite	V15 NABK	V15 BALCO	V16 NABK	V16 BALCO	V17 NABK	V17 BALCO
Wind speed	knots	12	12	3	3	5	5
Height of *T*gt (rel. gun)	m	−50.743425	−50.74342485	−7.5929532	−7.592953244	−82.265656	−82.2656558
Slant angle	gun mils	−88.888889	−88.88888889	−17.777778	−17.77777778	−124.44444	−124.4444444
Azimuth to target	gun mils	2933	2933	3022	3022	2133	2133
Target altitude	m	99	99	112	112	23	23
Quadrant elevation	gun mils	−82.64	−82.5777	−13.70	−13.6711	−117.04	−116.9777
Quadrant elevation	mrads	−81.14	−81.0705	−13.45	−13.4216	−114.90	−114.8426
Quadrant elevation	(°)	−4.65	−4.65	−0.77	−0.77	−6.58	−6.58
Super elevation	(°)	0.35	0.36	0.23	0.23	0.42	0.42
Super elevation	**mrads**	**6.13**	**6.20**	**4.01**	**4.03**	**7.27**	**7.33**
Azimuth of fire	gun mils	2930.97	2930.64	3022.425	3022.17	2132.16	2131.85
Azimuth of fire	mrads	2877.48	2877.15	2967.26	2967.01	2093.24	2092.94
Total drift angle	gun mils	2.36	2.36	−0.20	−0.17	1.17	1.15
Total drift angle (Coriolis on, wind on, spin on)	**mrads**	**2.32**	**2.31**	**−0.20**	**−0.17**	**1.15**	**1.13**
Time of flight	s	0.92	0.92	0.64	0.64	1.11	1.11
MV corrected for PT	$(m\cdot s^{-1})$	821.13	821.13	823.93	823.93	826.80	826.80
Velocity at impact	$(m\cdot s^{-1})$	487.659	487.22	560.00	559.48	449.45	448.94
Transonic entry distance	m	None	None	None	None	None	None
Transonic exit distance	m	None		None		None	
Maximum ordinate	m	0.00	0.0000	0.00	0.0000	0.00	0.0000
Range to max ordinate	m	0.00	0.0000	0.00	0.0000	0.00	0.0000
Azimuth of fire (Coriolis off)	gun mils	2931.02	2930.69	3022.46	3022.21	2132.18	2131.87
Azimuth of fire (Coriolis off)	mrads	2877.51725	2877.193565	2967.29022	2967.0439	2093.26184	2092.953864
Drift angle due to coriolis	gun mils	−0.04	−0.04	−0.03	−0.03	−0.02	−0.02
Drift angle due to coriolis	mrads	−0.04	−0.04	−0.03	−0.03	−0.02	−0.02
Azimuth of fire (Coriolis off, wind off)	gun mils	2933.21	2932.87	3022.14	3021.91	2133.18	2132.84
Azimuth of fire (Coriolis off, wind off)	mrads	2879.67	2879.34	2966.98	2966.76	2094.24	2093.91
Drift angle due to bullet spin	gun mils	0.13	0.13	0.09	0.09	0.15	0.16
Drift angle due to bullet spin	mrads	0.13	0.13	0.08	0.08	0.15	0.15
Drift due to wind	gun mils	2.27	2.27	−0.25	−0.23	1.03	1.02
Drift due to wind	mrads	2.23	2.23	−0.25	−0.22	1.02	1.00

The temperature is used to calculate the flight Mach numbers which in turn are used to extract the aerodynamic coefficients. Thus for large temperature differences, one expects significant discrepancies in the aerodynamic coefficients, such as the drag

Table 10
Results for vignettes 18, 19 and 20.

Variables	Unite	V18 NABK	V18 BALCO	V19 NABK	V19 BALCO	V20 NABK	V20 BALCO
Wind speed	knots	2	2	2	2	15	15
Height of *Tgt* (rel. gun)	m	−12.218545	−12.21854545	−84.083388	−84.08338821	−29.718895	−29.71889508
Slant angle	gun mils	−17.777778	−17.77777778	−106.66667	−106.6666667	−71.111111	−71.11111111
Azimuth to target	gun mils	1244	1244	1956	1956	5778	5778
Target altitude	m	591	591	1556	1556	80	80
Quadrant elevation	gun mils	−10.03	−9.9378	**−97.31**	−97.1021	**−67.45**	−67.4133
Quadrant elevation	mrads	−9.85	−9.7564	−95.54	−95.3298	−66.22	−66.1828
Quadrant elevation	(°)	−0.56	−0.56	−5.47	−5.46	−3.79	−3.79
Super elevation	(°)	0.44	0.44	0.53	0.54	0.21	0.21
Super elevation	**mrads**	**7.60**	**7.70**	**9.18**	**9.39**	**3.60**	**3.63**
Azimuth of fire	gun mils	1244.467	1244.04	**1955.11**	1955.59	**5777.91**	5778.12
Azimuth of fire	mrads	1221.75	1221.33	1919.42	1919.89	5672.45	5672.66
Total drift angle	gun mils	−0.02	−0.04	0.45	0.41	−0.13	−0.12
Total drift angle (Coriolis on, wind on, spin on)	**mrads**	**−0.02**	**−0.04**	**0.44**	**0.40**	**−0.13**	**−0.12**
Time of flight	s	1.17	1.17	**1.40**	**1.41**	**0.60**	**0.60**
MV corrected for PT	($m \cdot s^{-1}$)	829.75	829.75	832.15	832.15	835.22	835.22
Velocity at impact	($m \cdot s^{-1}$)	435.842	433.29	**402.65**	**394.62**	**594.63**	**593.83**
Transonic entry distance	m	None	None	**729.19**	767.5 DR($v = 408$ m/s)	None	None
Transonic exit distance	m	None		None		None	
Maximum ordinate	m	0.00	0.0000	0.00	0.0000	0.00	0.0000
Range to max ordinate	m	0.00	0.0000	0.00	0.0000	0.00	0.0000
Azimuth of fire (Coriolis off)	gun mils	1244.48	1244.06	1955.10	1955.58	5777.91	5778.12
Azimuth of fire (Coriolis off)	mrads	1221.76146	1221.350202	1919.41297	1919.88755	5672.44791	5672.655161
Drift angle due to coriolis	gun mils	−0.01	−0.02	0.01	0.01	0.00	0.00
Drift angle due to coriolis	mrads	−0.01	−0.02	0.01	0.01	0.00	0.00
Azimuth of fire (Coriolis off, wind off)	gun mils	1244.28	1243.84	1955.36	1955.80	5777.70	5777.92
Azimuth of fire (Coriolis off, wind off)	mrads	1221.57	1221.13	1919.67	1920.10	5672.24	5672.46
Drift angle due to bullet spin	gun mils	0.16	0.16	0.20	0.20	0.08	0.08
Drift angle due to bullet spin	mrads	0.16	0.16	0.19	0.20	0.08	0.08
Drift due to wind	gun mils	−0.17	−0.19	0.25	0.20	−0.21	−0.21
Drift due to wind	mrads	−0.17	−0.18	0.24	0.20	−0.21	−0.20

Table 11
NABK-BALCO differences in QE, SE.

	QE NABK/(°)	QE BALCO/(°)	Magnitude of difference in QE/(°)	SE NABK/(°)	SE BALCO/(°)	Magnitude of difference in SE/(°)
V1	−0.08	−0.07	0.0014	0.42	0.43	0.0014
V2	−0.43	−0.44	0.0045	1.57	1.56	0.0045
V3	20.82	20.83	0.0098	0.82	0.83	0.0098
V4	−2.31	−2.31	0.0034	0.69	0.69	0.0034
V5	−11.35	−11.35	0.0058	0.65	0.65	0.0058
V6	−5.75	−5.75	0.0023	0.25	0.25	0.0023
V7	−2.74	−2.74	0.0009	0.26	0.27	0.0009
V8	−9.79	−9.79	0.0013	0.21	0.21	0.0013
V9	−29.82	−29.82	0.0013	0.18	0.18	0.0013
V10	1.32	1.32	0.0028	0.32	0.32	0.0028
V11	0.90	0.91	0.0071	0.90	0.91	0.0071
V12	15.46	15.46	0.0028	0.46	0.46	0.0028
V13	11.09	11.10	0.0041	1.09	1.10	0.0041
V14	−0.72	−0.72	0.0005	0.28	0.28	0.0005
V15	−4.65	−4.65	0.0037	0.35	0.36	0.0037
V16	−0.77	−0.77	0.0014	0.23	0.23	0.0014
V17	−6.58	−6.58	0.0034	0.42	0.42	0.0034
V18	−0.56	−0.56	0.0054	0.44	0.44	0.0054
V19	−5.47	−5.46	0.0118	0.53	0.54	0.0118
V20	−3.79	−3.79	0.0020	0.21	0.21	0.0020

coefficient. Furthermore, the difference in temperature is expected to significantly impact velocity at the target with a relatively large separation between the shooter and the target. With vignette 19, the range was relatively long at 800 m. This only exacerbated the difference in projectile performance as obtained with NABK and BALCO.

The differences in total drift angles obtained with NABK and BALCO for all vignettes are shown in Table 13. The maximum difference is 0.13 mils, or 0.0073°, obtained with vignette 11, and the second largest is 0.09 mils, obtained with vignettes 4 and 5. The average NABK-BALCO difference in total drift angle is 0.04 mils.

In case of projectile drift due to Coriolis effects, wind and bullet spin, the results of the comparison between NABK and BALCO are presented in Table 14. Magnitude of the difference between drift due to Coriolis obtained with NABK and BALCO is the largest for vignette 18 (rounded value of 0.009 mils). Magnitude of the difference between drift due to projectile spin obtained with NABK and BALCO is the largest for vignette 2 (rounded value of 0.027 mils). Magnitude of the difference between drift due to wind effects obtained with NABK and BALCO is the largest for vignette 11

Table 12
NABK-BALCO differences in velocity at impact.

	NABK velocity at impact/ ($m \cdot s^{-1}$)	BALCO velocity at impact/ ($m \cdot s^{-1}$)	Magnitude of difference in velocities at impact/ ($m \cdot s^{-1}$)	Percentage error with respect to BALCO magnitude
V1	391.77	392.0360	0.26	0.07
V2	253.33	254.37	1.04	0.41
V3	272.966	273.25	0.28	0.10
V4	320.14	319.45	0.69	0.22
V5	320.66	319.94	0.72	0.23
V6	527.84	527.28	0.56	0.11
V7	515.20	516.62	1.42	0.27
V8	553.62	553.49	0.12	0.02
V9	584.98	584.43	0.54	0.09
V10	474.20	474.64	0.44	0.09
V11	308.12	307.99	0.13	0.04
V12	420.22	420.00	0.21	0.05
V13	298.25	298.32	0.07	0.02
V14	513.72	513.48	0.24	0.05
V15	487.659	487.22	0.44	0.09
V16	560.00	559.48	0.52	0.09
V17	449.45	448.94	0.50	0.11
V18	435.842	433.29	2.55	0.59
V19	402.65	394.62	8.03	2.04
V20	594.63	593.83	0.80	0.13

Table 13
NABK-BALCO differences in total drift angles.

	Total drift angle NABK/mils	Total drift angle BALCO/mils	Magnitude of total drift angle difference/mils
V1	−2.66	−2.69	0.03
V2	−4.56	−4.59	0.03
V3	−3.75	−3.80	0.05
V4	4.06	3.97	0.09
V5	4.15	4.06	0.09
V6	1.49	1.55	0.06
V7	0.78	0.74	0.04
V8	−0.33	−0.37	0.04
V9	0.44	0.45	0.01
V10	−2.98	−3.05	0.07
V11	−1.40	−1.53	0.13
V12	−1.14	−1.18	0.04
V13	0.43	0.44	0.01
V14	−1.26	−1.27	0.01
V15	2.36	2.36	0.00
V16	−0.20	−0.17	0.03
V17	1.17	1.15	0.02
V18	−0.02	−0.04	0.02
V19	0.45	0.41	0.04
V20	−0.13	−0.12	0.01

Table 14
NABK-BALCO differences in drift angles.

	Drift due to Coriolis NABK/ mils	Drift due to Coriolis BALCO/ mils	Drift due to spin NABK/ mils	Drift due to spin BALCO/ mils	Drift due to wind NABK/ mils	Drift due to wind BALCO/ mils	Difference in drift due to Coriolis/mils	Difference in drift due to spin/mils	Difference in drift due to wind/mils
V1	−0.06	−0.06	0.17	0.17	−2.77	−2.79	0.000	0.005	0.024
V2	−0.16	−0.16	0.65	0.67	−5.04	−5.10	0.001	0.027	0.060
V3	−0.08	−0.08	0.41	0.41	−4.08	−4.13	0.000	0.004	0.052
V4	−0.09	−0.09	0.28	0.28	3.86	3.77	0.000	0.001	0.093
V5	−0.09	−0.09	0.27	0.27	3.98	3.88	0.001	0.001	0.092
V6	−0.03	−0.03	0.09	0.09	1.43	1.49	0.000	0.004	0.060
V7	−0.04	−0.04	0.10	0.10	0.72	0.68	0.000	0.000	0.036
V8	−0.03	−0.03	0.08	0.08	−0.38	−0.42	0.000	0.003	0.043
V9	0.04	0.04	0.07	0.07	0.33	0.34	0.003	0.000	0.011
V10	−0.03	−0.03	0.13	0.13	−3.08	−3.15	0.001	0.000	0.072
V11	0.04	0.04	0.35	0.35	−1.79	−1.93	0.001	0.005	0.137
V12	−0.07	−0.07	0.17	0.17	−1.24	−1.28	0.000	0.002	0.037
V13	0.00	0.00	0.43	0.44	−0.01	0.00	0.002	0.006	0.007
V14	0.03	0.03	0.11	0.11	−1.40	−1.41	0.000	0.000	0.010
V15	−0.04	−0.04	0.13	0.13	2.27	2.27	0.001	0.001	0.004
V16	−0.03	−0.03	0.09	0.09	−0.25	−0.23	0.000	0.000	0.025
V17	−0.02	−0.02	0.15	0.16	1.03	1.02	0.001	0.002	0.019
V18	−0.01	−0.02	0.16	0.16	−0.17	−0.19	0.009	0.001	0.012
V19	0.01	0.01	0.20	0.20	0.25	0.20	0.001	0.006	0.043
V20	0.00	0.00	0.08	0.08	−0.21	−0.21	0.000	0.000	0.006

(rounded value of 0.137 mils). The average difference NABK-BALCO in projectile drift due to Coriolis effects is 0.0012 mils, that due to projectile spin is 0.0034 mils, and that due to wind is 0.0422 mils (using rounded values for the calculation of the average). On average, wind has the largest impact on drift size among the three factors considered.

9. Conclusion

This report provides an assessment of NATO Armaments Ballistic Kernel (NABK) firing solutions for a number of relevant sniper vignettes for the NATO 7.62 × 51 mm, OTBT,168 gr, Match ammunition. The work presented in this report is the first known validation of NABK data for sniper vignettes. The direct fire trajectory simulation study indicates that the results, mainly about the fire control inputs and the resulting drift, of the 6-degree-of-freedom simulations of the NATO 7.62 × 51 mm, OTBT,168 gr Match ammunition projectile in BALCO are in close agreement to those obtained with the 4-degree-of-freedom simulations in NABK for all the vignettes investigated. The largest observed difference between the various parameters compared was 2% for the terminal velocity in vignette 19. Typical difference in terminal velocity was less than 0.5%.

For the vignettes studied, the fire control inputs for BALCO and NABK resulted, in practically the same impact point for both trajectory algorithms. Relying on the BALCO-NABK comparison results presented in this paper, it is concluded that NABK is sufficiently accurate to predict the trajectory of direct fire small caliber projectiles. Therefore, the use of NABK for a sniper ballistic computer can be recommended.

References

[1] Sowa, A.J., "NATO Shareable Software Developing Into True Suite Supporting National Operational, Fire Control Systems" in proceedings of the 24th International Symposium on Ballistics, New Orleans, LA, September 22-26, 2008.
[2] Chusilp, P, Charubhun, Weerawut and Ridluan, A., "Developing Firing Table Software for Artillery Projectiles using Iterative Search and 6-DOF Trajectory Model", in proceedings of the 2nd TSME International Conference on Mechanical Engineering, Krabi, Thailand, October 19-21, 2011.
[3] Ortac, S.A., Durak, U., Kutluay, U., Kucuk, K. and Candan, C., "NABK Based Next Generation Ballistic Table Toolkit", in proceedings of the 23rd International Symposium on Ballistics, Tarragona, Spain, April 16-20, 2007.
[4] The Modified Point Mass and Five Degrees of Freedom Trajectory Models. NATO STANAG 4355. Edition 3 2009.
[5] Wey, P., Corriveau, D., Saitz, T.A., de Ruijter, W. and Strömbäck, P., "BALCO 6/7-DoF trajectory Model" in proceedings of the 29th International Symposium on Ballistics, Edinburgh, UK, May 9-13, 2016.
[6] The Six/Seven Degrees of Freedom Guided Projectile Trajectory Model. NATO STANREC 4618. Edition 1 January 2014.
[7] McCoy RL. Modern Exterior Ballistics – the launch and flight dynamics of symmetric projectiles. Schiffer Military History; 1999.
[8] Guide for the verification and validation of computational fluid dynamics simulations. AIAA G-077–1998; 1998.